

Article

Monitoring and Evaluation of Sandstone Decay Adopting Non-Destructive Techniques: On-Site Application on Building Stones

Teresa Salvatici *[†], Sara Calandra [†], Irene Centauro [†], Elena Pecchioni [†], Emanuele Intriери [†]
and Carlo Alberto Garzonio [†]

Department of Earth Sciences, University of Florence, Via A. La Pira 4, 50125 Florence, Italy;
sara.calandra@stud.unifi.it (S.C.); irene.centauro@unifi.it (I.C.); elena.pecchioni@unifi.it (E.P.);
emanuele.intriери@unifi.it (E.I.); carloalberto.garzonio@unifi.it (C.A.G.)

* Correspondence: teresa.salvatici@unifi.it

† These authors contributed equally to this work.

Received: 2 October 2020; Accepted: 5 November 2020; Published: 6 November 2020



Abstract: This paper focuses on the characterization approach to evaluate the decay state of *Pietra Serena* of historic buildings in Florence (Italy). *Pietra Serena* is a Florentine sandstone largely used in the city especially during the Renaissance; it is a symbol of cultural heritage of Florence and constitutes a large part of the city center, which was named a World Heritage Site by UNESCO in 1982. Unfortunately, many environmental factors negatively affect the stone, increasing damage and the danger of falling material. Any detachment of stone fragments, in addition to constitute a loss in cultural heritage, can be dangerous for citizens and the many tourists that visit the city. The use of non-destructive techniques (NDTs) as ultrasonic and Schmidt hammer tests can quantitatively define some mechanical properties and help to monitor the decay degree of building stone. In this study, the NDTs were combined with mineralogical, petrographical, chemical and physical analyses to investigate the stone materials, in order to correlate their features with the characteristics of the different artefacts in *Pietra Serena*. Correlations between the NDTs results and the compositional characteristics of the on-site stone were carried out; such discussion allows to identify zones of weakness and dangerous unstable elements.

Keywords: NDT; decay; cultural heritage; *Pietra Serena*

1. Introduction

In Florence (Italy) and its surroundings, *Pietra Serena*, an easily workable sandstone outcropping nearby the city, has been mainly exploited for ornamental purposes. Its employment flourished during the Renaissance but its use continued until the 19th Century. The recognition of the value of the architectural elements in *Pietra Serena* has drawn attention to the importance of preserving these artefacts since their life can be drastically curtailed when they are exposed to decay processes.

A stone placed in different environmental conditions (pressure, temperature, etc.) from those where it formed tends to reach new conditions of equilibrium through changes in its characteristics, which means that the stone begins to degrade. Clearly, this depends on its lithological features invariably combined with physical, biological and chemical processes due to environmental factors. Moreover, in urban areas, building materials situated in the open air, in addition to the natural decay, are affected by the action of atmospheric pollutants [1–4].

In this paper, we focus on stone corbels placed below balconies and eaves, architectonic elements permanently exposed to weather, placed in urban areas. Indeed, in addition to having a decorative function, these elements also have an important structural function. Over time, this exposure involves modifications of the intrinsic stone characteristics leading to a loss in terms of mechanical properties or to the impairment of use. Therefore, the corbels themselves can influence the mechanics, as they carry significant weights. Monitoring the state of damage and mechanical properties of these structural architecture elements means evaluating the performance of the support structure.

The aim of this paper is to improve the knowledge on *Pietra Serena* in architecture and cultural heritage conservation alike and to characterize the decay degree of stone architectonic elements using non-destructive techniques (NDTs), namely the ultrasonic and Schmidt hammer tests. This assessment is also fundamental in the light of the Santa Croce Basilica tragedy happened on 19 October 2017, when a visitor died because of a stone corbel falling from the ceiling as well as in light of other similar events, with less dramatic consequences, occurred in the Florentine area.

The ultrasonic and the Schmidt hammer tests are chosen to define the mechanical properties of materials and the weathering state of building stones [5–9]. In particular, these tests enable to calculate the uniaxial strength of the rock through a correlation with the velocity of P-waves (V_p) travelling throughout the stone or with the rebound value (R) of a spring-loaded mass impacting against the surface, respectively. The portability of the instrumentation allows the operators to perform on-site diagnostic campaigns, making these techniques a popular solution for monitoring.

The corbels of five case studies were investigated with NDTs. For each case, a corbel was selected for sampling and described with the visual weathering evaluation method according to the ICOMOS International Scientific Committee for Stone (ISCS) illustrated glossary [10].

The selected corbels were used to understand how mineralogical, petrographical, chemical, physical features and the different state of decay influence the NDTs results. Then, a correlation between V_p and R was developed to obtain a new approach that can improve the diagnostic process on Florentine sandstone in cultural heritage applications.

2. Florentine *Pietra Serena* Sandstone

Corbels used to adorn balconies or eaves are characterized by different sizes and may be simply or richly carved; typically, they are made of a Florentine blue-grey colored (when freshly cut) sandstone of medium strength and easy to work, called *Pietra Serena* (“the stone with the color of the sky”). For this reason, it was widely employed mainly in the Renaissance as decorative and ornamental material in the monuments of Florence [11–13].

Pietra Serena is the commercial/artistic name of a sandstone that originally belongs to the Macigno/Monte Modino Formations (Upper Oligocene/Lower Miocene), cropping out in the Northern Apennines [14,15]. *Pietra Serena* extracted from these formations can be defined as a medium-coarse-grained lithic arkose with a prevailing clay matrix [13,16].

However, it is necessary to emphasize that, over the years, the request for *Pietra Serena* was so high that sometimes it was necessary to use other sandstones belonging to different geological formations and with slightly different characteristics from the original *Pietra Serena*: e.g., the sandstone coming from Monte Senario Formation, a feldspathic/lithic medium-coarse and sometimes medium-fine sandstone, with a binder mainly constituted by clay with a non-negligible quantity of calcite cement [17]. Another surrogate is Firenze sandstone, which is macroscopically similar to *Pietra Serena* but belongs to the Marnoso–Arenacea Formation and is characterized by a mineralogical and petrographical heterogeneity that strongly affects its physical and mechanical parameters [18].

As mentioned above, in general, the decay of stones depends on intrinsic parameters, like composition and textural/structural characteristics, and on extrinsic agents, like climate and anthropic work. Changes in temperature are a very important factor to be considered, since they can cause microfractures that can increase sandstone’s porosity and enable penetration of rainwater, water vapor etc., which further contributes to the degradation, thus triggering a self-feeding loop [19,20].

In fact, in *Pietra Serena*, the rainwater and the air humidity play a fundamental role in the decay, accelerating the process: water can induce volumetric expansion of the crystal lattices (clay minerals of the matrix) and lead to consequent exfoliation and granular disintegration of the stone followed by contour scaling, until the loss of material. Water can also act mechanically by removing the clay matrix and leaving the stone completely disaggregated and with a dusty appearance. Water can also dissolve the calcite cement, increasing the porosity inside the stone. Consecutively, in the evaporation phase, the dissolved calcite can precipitate on the external surface forming up to one-centimeter-thick crusts, with low permeability; these crusts may be weakly bonded to the substrate and can often detach completely. Finally, on icy days, the water absorbed at a certain depth freezes and further widens the cracks, while the rise of temperature causes the thawing of the outer parts of block (cyclic freezing-thawing). Repeated cycles cause changes in the characteristics of the original rock, leading to significant increase in initial porosity, resulting in weaker areas [21–23].

3. Sites Description

Analyses on *Pietra Serena* corbels belonging to five monuments in Florence city center were carried out. They have both a decorative function, and an important structural utility.

The five case studies represent important historical buildings and churches (Figure 1): Corsini al Prato Palace, Ginori Conti Palace, Santa Croce Basilica, Medici Riccardi Palace and Santissima Annunziata Basilica. In Table 1 the description of the most degraded corbel for each case, therefore chosen for sampling, is reported.

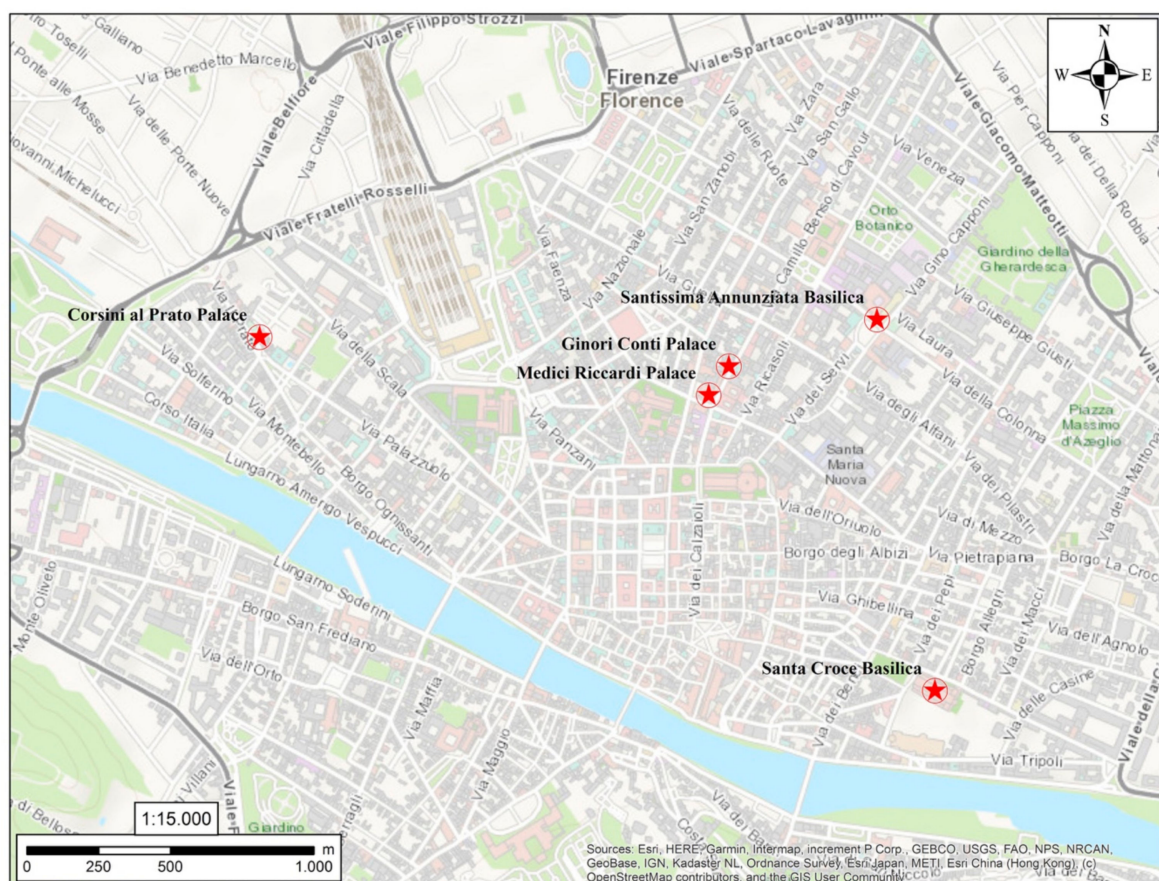


Figure 1. Map of Florence with the location of the case studies.

Corsini al Prato Palace (CP) was designed in 1591 and, over time, many interventions have been carried out. During the 19th century the building was enlarged following the purchase of adjacent land. Among the changes, the two balconies of the palace's façade were inserted: one supported by four corbels and one by 18 corbels. All elements (22) were investigated. They are exposed in open air, in a north-west/south-east direction. These artefacts present a varying degree of damage. The lateral areas of the balconies (in particular the two corbels at the end of the first balcony, and two on the right hand side and four on the left hand side of the second), given their higher exposure to the rain and atmospheric pollutants, are the most vulnerable. The level of decay was so high that, in 2018, a lateral corbel of the second balcony fell off. All the other corbels are in good state of preservation.

Table 1. Decay description of the corbels in studied sites.

CORBELS	Crack and Deformation	Detachment	Material Loss	Discoloration and Deposit	Biological Colonization
	Fracture	Delamination Disintegration Fragmentation Contour scaling	Erosion Missing part	Patina Encrustation Efflorescence	Lichen
	Crack	-	Erosion Missing part	Crust Deposit Efflorescence	-
	Crack Fracture	Exfoliation Disintegration Contour scaling	Erosion Pitting Missing part	-	-
	-	Disintegration Contour scaling	Pitting	-	-
	Microfissures	Disintegration Contour scaling	Pitting	-	-

The corbels are characterized by the granular disintegration of the stone and the presence of surface deposits. The loss of material depends on the high weathered state of the stone.

The sandstone elements on the façade show color changes (mainly red-brown) due to the development of an iron-rich patina, as a result of the oxidation of Fe^{2+} as a consequence of particular condition of decay, such as the presence of water, CO_2 and the low pH [16]. In Table 1a the description of the most degraded corbel is reported.

Ginori Conti Palace (GC) was built in the mid-18th Century on the ancient properties of the Medici family that once ruled Florence (from XV to XVIII centuries); the building has a balcony on the second level of the façade, supported by four stone corbels located in the open air and exposed in a north-south direction. The four corbels were investigated. During a previous restoration campaign,

mortar was added to improve the adhesion of the corbels to the balcony and avoid the detachment of material. Such a finishing layer prevents from having a complete vision of the underlying stone, the visual complete analysis of its degradation impossible. It is reported that in 2019 a corbel has fallen: a structural problem of the balcony, run-off water and significant variations in the environmental parameters caused a deep fracture, which over time led to its complete fall.

The other corbels do not show any evident fractures, with the mortar well linked to the base stone (Table 1b).

Santa Croce Basilica (SC) is the principal Franciscan church in Florence, located at the eastern side of Santa Croce square. The construction of the current church, to replace an older building, was begun in 1294, possibly by Arnolfo di Cambio, and it was consecrated in 1443. The interior of Santa Croce is characterized by a wide central nave and two lateral ones. The Basilica has a “*commissa*” cross plan characterized by a particularly large transept preceding the polygonal apse. The *Pietra Serena* element studied is one of the corbels (denominated “*peduccio*”) on which the trussed roof of the right transept was placed (Table 1c). Such corbel concerns the 19 October 2017 tragedy, when the element fell off on a visitor of the church and killed him. This is the only case, in our study, of a corbel not exposed to external weathering. Although it is kept indoors, the corbel is in a poor state of conservation and is characterized by intense decay, numerous cracks, exfoliation and advanced decohesion, as a probable consequence of a continuing exposure to masonry moisture caused by internal percolations of rainfall.

Medici Riccardi Palace (MR) is a Renaissance palace, designed by Michelozzo di Bartolomeo for Cosimo de’ Medici between 1444 and 1484. It was well known for its stone masonry, which includes architectural elements: rusticated blocks on the ground floor, the ashlar faces of the top story, and the cornice. The building overlooks de’ Gori street (east-west direction) and C. Cavour street (north-south direction). A total of 86 elements below the eaves, on both sides of the Riccardi Medici building were investigated, of which 55 on the north-south façade and 31 on the east-west façade. The corbels are, in general, in a good state of conservation, superficial lesions are absent, and the detachment is very low. During the recent restoration, some elements have shown slight contour scaling, (see example in Table 1d): such corbel is in good condition with a scarce pitting.

The Santissima Annunziata Basilica (SSA) was founded in 1250, located at the north-eastern side of the Santissima Annunziata square. In the mid-15th Century the external portico, composed of an arch, was added by Antonio Manetti, to conform to the Renaissance characters of the square. In the 17th Century Giovanni Battista Caccini extended the arcade of the Basilica. Below the eaves, there is a series of well carved stone corbels, of which 14 elements were investigated. In general, these elements are in a good state of conservation, similarly to the MR case. In Table 1e the decay description of the corbel that has suffered the most degradation is indicated.

4. Analytical Methods

In this study, the experimental research was carried out in two stages: on-site and in laboratory. About the on-site analyses, the NDTs measurements of V_p and R were performed on all corbels of the monuments. For the laboratory tests, the specimens were taken from stone pieces sampled from the corbels described in Table 1, that had fallen from the monuments and could not be used again as part of any restoration, only in the cases of CP and SC the samples were taken from fallen corbels. For the physical analyses 5 specimens of $2 \times 2 \times 2$ cm were cut from CP and SC corbels, while for the other study cases only 3 were cut. The mineralogical and chemical analyses were carried out on the powdered samples; while for the petrographic analysis, 2 scales were selected for the preparation of the thin sections.

4.1. NDT Techniques Application

The NDT methods, such as the ultrasonic velocity and Schmidt hammer tests, are widely employed to investigate the mechanical properties of many materials [5,24–26]. In particular, they can provide a valuable contribution in monitoring and evaluating the state of deterioration of building stones.

NDTs are applied to clarify the level of damage, the presence of defects, cracks and weathering effects, without taking samples of material.

The ultrasonic testing is based on the acoustic properties of different materials. A piezoelectric probe generates ultrasonic waves. The velocity of the first wave able to travel through the rock material (V_p) is calculated by measuring the travel time (t) and the distance between transmitter and receiver (L):

$$V_p = \frac{L}{t} \quad (1)$$

V_p value is closely related to the physical properties of the material, such as density, elasticity, porosity, and water content. The propagation velocity also depends on the state of conservation of the stone and on the presence of concealed inhomogeneity and detachments, both superficial and internal [27–31].

In this study, 2 ultrasonic instruments were used: TICO equipment from Proceq and IMG 5200 CSD, with a resonance frequency of 54 kHz and 50 kHz, respectively.

The tests on the *Pietra Serena* corbels were performed with accuracy of $\pm 1\%$ in direct transmission mode, meaning that the transmitter and receiver were placed on opposite and parallel faces. The effectiveness of the test increases with smooth and flat surfaces [32], therefore, to improve smoothness, a thin layer of aqueous coupling gel, reversible and harmless, is spread on the stone.

On each corbel, where possible, the measurements were carried out both in the central and in the outermost portion, to verify the uniformity of the entire element.

The Schmidt hammer test, originally designed for testing the hardness of concrete, has been widely used for estimating the mechanical properties of many different rock types [33] and for the assessment of weathered stone hardness [34,35]. It is a minimally invasive test and is particularly effective in assessing the quality of the surfaces of stone elements.

This method involves the use of an instrument, the Schmidt hammer, which measures the rebound value (R), which refers to the resistance of the surface to successive n impacts of the hammer plunger. R values depend on the hardness of the surface and many other factors (type and orientation of the hammer, dimensions of the sample, smoothness of the surface, inclination of the hammer with respect to the surface) [36]. The working principles of the Schmidt hammer are shown in detail by [37] and the standard test method is described in [38].

For this work, 2 Schmidt hammers were used: N-type 58-C0181/N by Controls Group and L-type Geostone by Novatest. At least 3 rebounds were performed on about 10 different points on each surface of the corbels corresponding to the same areas investigated with the ultrasonic test. The hammer was always kept perpendicular to the plane in order to minimize the error in the measurement due to the inclination of the instrument. The average values of R were obtained from these measurements. This method provides the better estimation of the surface hardness of the material [39].

4.2. Laboratory Tests

The petrographic observations on thin sections of 30 μm of thickness [40], were carried out by means of a ZEISS Axio Skope.A1 microscope, with a video camera, 5 Megapixel of resolution and image analysis software AxioVision [41]. To identify the mineralogical composition of the samples, X-ray Powder Diffraction (XRPD) was used. A Philips PW 1050/37 diffractometer was utilized with a Panalytical X'Pert PRO and High Score software data acquisition and interpretation system, operating at 40 kV–20 mA, with a Cu anode, a graphite monochromator and with $2^\circ/\text{min}$ goniometry speed in a scanning range between 5° – $70^\circ\theta$; the slits are 1-01-1 and the detection limit is 4% [42–44].

The amount of CaCO_3 was determined with a gasometric method [45] using the Dietrich-Frühling calcimeter. The percentage of calcite was calculated with reference to a calibration curve constructed by linking the volume of CO_2 developed by the acid attack of the powdered rock with the amount of pure CaCO_3 .

Laboratory testing, including apparent density, open porosity and imbibition coefficient, was carried out on the prismatic specimens cut from stone pieces sampled [18,46,47].

Bulk density, open porosity and imbibition coefficient were calculated with Hydrostatic balance Mettler Toledo XS 204 with a maximum weight 220 g and a precision of 0.001 g. Only distilled water was used. The specimens were dried in an oven at $60 \pm 5^\circ \text{C}$ until a constant mass was reached (m_{dry}). To maintain m_{dry} , the samples were kept in a desiccator when cooling down to room temperature.

In a typical procedure, the samples are placed in distilled water inside a crystallizer. To obtain wet weight (m_{wet}), the specimens are measurement after a week and then at regular daily intervals to verify that they are completely saturated. With this technique the imbibition coefficient (CI) is evaluated through the weight, with the following equation:

$$\text{CI} = \left(\frac{m_{\text{wet}} - m_{\text{dry}}}{m_{\text{dry}}} \right) * 100 \quad (2)$$

A further in-depth analysis of imbibition is provided by measuring the hydrostatic weight (m_{hyd}) and with it the apparent density and volume of the samples and therefore the open porosity, through the application of relationships between the different weights.

The apparent density is:

$$\rho = \frac{m_{\text{wet}}}{m_{\text{wet}} - m_{\text{hyd}}} (\rho_0 - \rho_L) + \rho_L \quad (3)$$

where ρ_0 is the air density and ρ_L the density of the liquid, in this case distilled water.

The porosity accessible to water, or open porosity, is expressed by the percentage ratio between the volume of open pores and the apparent volume of the specimen, according to the following expression:

$$\phi = \left(\frac{m_{\text{wet}} - m_{\text{dry}}}{m_{\text{wet}} - m_{\text{hyd}}} \right) * 100 \quad (4)$$

5. Results and Discussion

The X-ray diffraction analyses highlighted for all the samples of *Pietra Serena* (Table 2) a typical composition constituted mainly by quartz and feldspars; calcite, micas and clay minerals are in lower amount; only in SC gypsum, probably of secondary origin due to the state of decay, was detected, while in SSA traces of iron oxides were found.

Table 2. Mineralogical analysis of the *Pietra Serena* sandstone.

Samples	Quartz	Calcite	Feldspars	Micas	Clay min.	Gypsum	Goethite
CP	xxx	tr	xx	tr	x	-	-
GC	xxx	x	xx	x	x	-	-
SC	xxx	x	xx	x	x	x	-
MR	xxx	x	x	x	x	-	-
SSA	xxx	x	x	x	x	-	tr

xxx = high content; xx = medium content; x = low content; tr = traces.

The petrographical analyses show in some samples (e.g., SC, and CP) a high state of decay with lack of the clay matrix, low amount of microsparitic calcite cement and presence of fractures; the sandstone shows clastic granules of medium coarse sizes constituted by quartz, feldspar fragments of metamorphic and magmatic rocks, muscovite and biotite often transformed into chlorite (Figure 2). Otherwise, in the cases of GC, SSA and MR, the sandstone shows a better condition of conservation, higher amount of microsparitic calcite cement and a higher compactness; the clastic granules are of medium-fine sizes always constituted by quartz, feldspars fragments of metamorphic and magmatic rocks, muscovite and biotite often transformed into chlorite (Figure 3). Mineralogical and petrographical

results suggest that the examined samples belong to different Florentine quarries of Macigno/Monte Modino Formations [13].

Table 3 gives an overview of the physical analysis results and shows the average values and variation coefficient measured for the five case studies. These values are probably related to the decay parameters determined in the monuments.

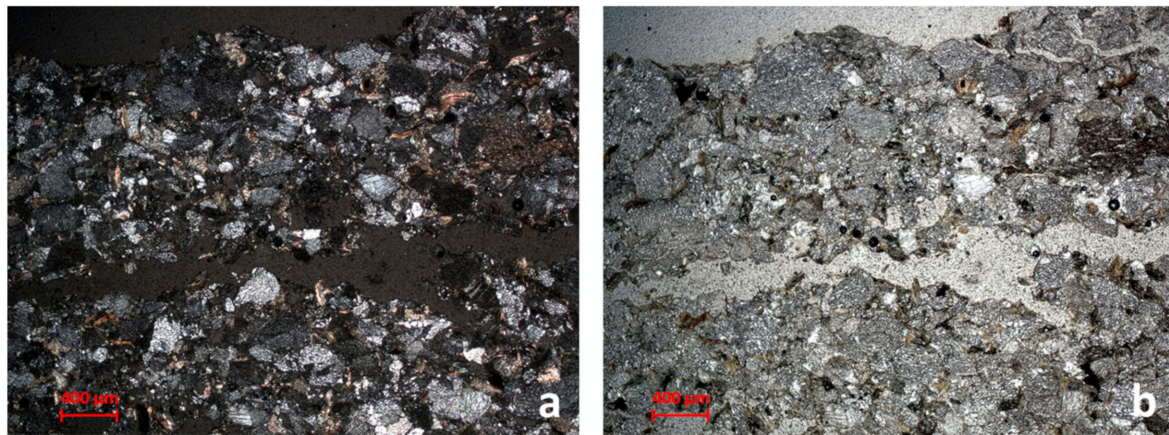


Figure 2. (a) SC sample image of the thin section in cross polarized light (xpl), showing the presence of cracks and fractures parallel to the surface; (b) image in plane polarized light (ppl) of the same sample where cracking and decohesion between the granules are evident.

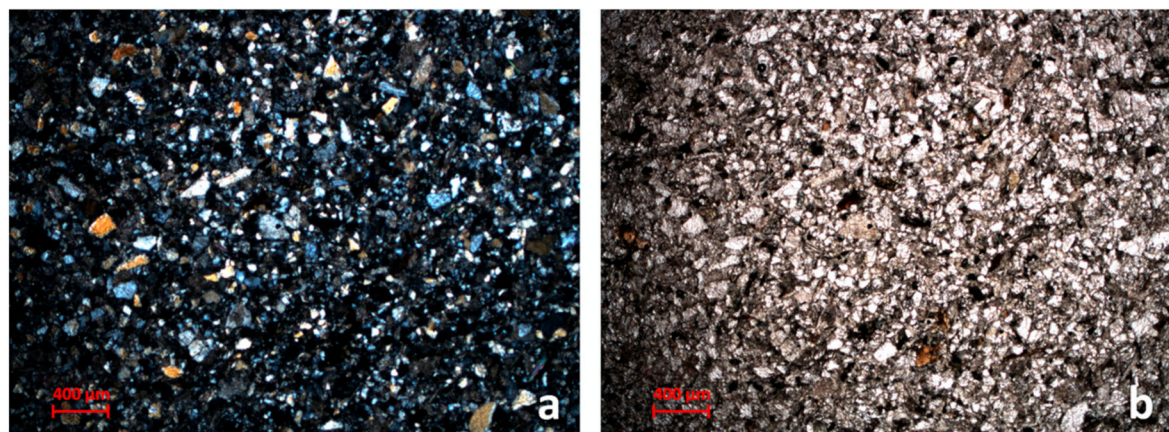


Figure 3. (a) GC sample image of the thin section in cross polarized light (xpl); (b) image in plane polarized light (ppl) of the same sample: in both images the medium-fine grain size of quartz and feldspars and the higher compactness of the rock are shown.

Table 3. Results of physical and gasometric analyses, ρ (g/cm^3) is the apparent density, CI (%) is the imbibition coefficient, ϕ (%) is open porosity and CaCO_3 (%) is calcium carbonate content.

Samples	ρ (g/cm^3)	CI (%)	ϕ (%)	CaCO_3 (%)
CP	2.616 ± 0.001	1.720 ± 0.042	4.436 ± 0.107	2.7
GC	2.651 ± 0.001	1.273 ± 0.017	3.341 ± 0.046	6.4
SC	2.528 ± 0.021	2.043 ± 0.192	5.097 ± 0.426	2.7
MR	2.638 ± 0.008	1.268 ± 0.037	3.317 ± 0.115	15.0
SSA	2.642 ± 0.003	1.137 ± 0.049	2.978 ± 0.130	10.7

SC samples show a higher open porosity and thus a higher CI. The apparent density is inversely proportional to the other factors and so the GC, MR and SSA samples show a low CI and ϕ . The percentage of CaCO_3 obtained by the gasometric analyses shows different amounts among the samples, being lower for CP and SC (Table 3). The state of decay of some samples (CP and SC) is evidenced by the low amount of clay minerals, which probably were lost as a result of the water washout, and also by the low amount of calcite and consequently higher porosity; on the other hand, GC, MR and SSA case studies exhibit a better state of conservation.

The results of the ultrasonic and Schmidt hammer tests are reported in Figure 4. By comparing the results of NDTs performed on corbels selected for sampling (in blue in Figure 4), a good correlation between the distribution of V_p and R values and laboratory tests results was observed.

It can be seen that the stone of SC is the lithotype characterized by the lowest V_p and R values, in fact it shows medium-coarse grain sizes of the clastic granules, higher porosity and a lower content of CaCO_3 than the others. These characteristics are related both to the presence of fractures parallel to the surface and to the decohesion between the granules, probably also due to the dissolution phenomena (see low content of calcite). Similarly, the CP corbel displays low values of V_p and R and in fact has a high porosity and a low content of CaCO_3 .

The corbels of GC, MR and SSA, instead, show high values of V_p and R, and present medium-fine grain size of the clastic granules, which makes the rock more compact with respect to the other cases. It should also be noted that the *Pietra Serena* of these case studies is characterized by a higher CaCO_3 content.

Considering the average values of V_p and R (Table 4), it is possible to note that the values obtained with the ultrasonic test are between 2200 and 3200 m/s in all the case studies, with the only exception of those measured on the corbel of SC (where only the fallen corbel was analyzed), which is largely below the average. Additionally, the Schmidt hammer test recorded average results, with R values comprised between 33 and 39, except for SC.

All corbels investigated are summarized in Figure 5, where the correlation between V_p and R is shown. The values distribution is linear and V_p is directly proportional to R, with a Pearson's correlation coefficient of $r = 0.83$. The red cluster represents low V_p and R values, correlated to decay and weakness zones of the corbels (in this area the corbels of CP, SC and only one corbel of SSA are represented). A comparison between the description of degradation forms (Table 1) and the results of V_p and R values shows that the *Pietra Serena* is characterized by very low V_p where a low R generally corresponds to degraded areas suffering from exfoliation with the relative loss of shallow material, and in some cases represents the fallen corbels or those at risk of falling.

Table 4. Ultrasonic and Schmidt hammer tests average values and standard deviations for each case study.

Case Studies	V_p (m/s)	R (-)
CP	2616 ± 1241	35 ± 9
GC	3217 ± 489	39 ± 8
SC	497 ± 143	22 ± 2
MR	2746 ± 533	36 ± 4
SSA	2932 ± 716	36 ± 7

The green cluster represents the high V_p and R values, which indicate a good state of preservation of *Pietra Serena* (in this area they are mainly represented by the corbels of GC and MR described above and also most of the corbels of SSA). The only case studies that are represented in both clusters are CP and, to a lesser extent, SSA. Such results are often due to the considerable variability of on-site corbels' state of conservation.

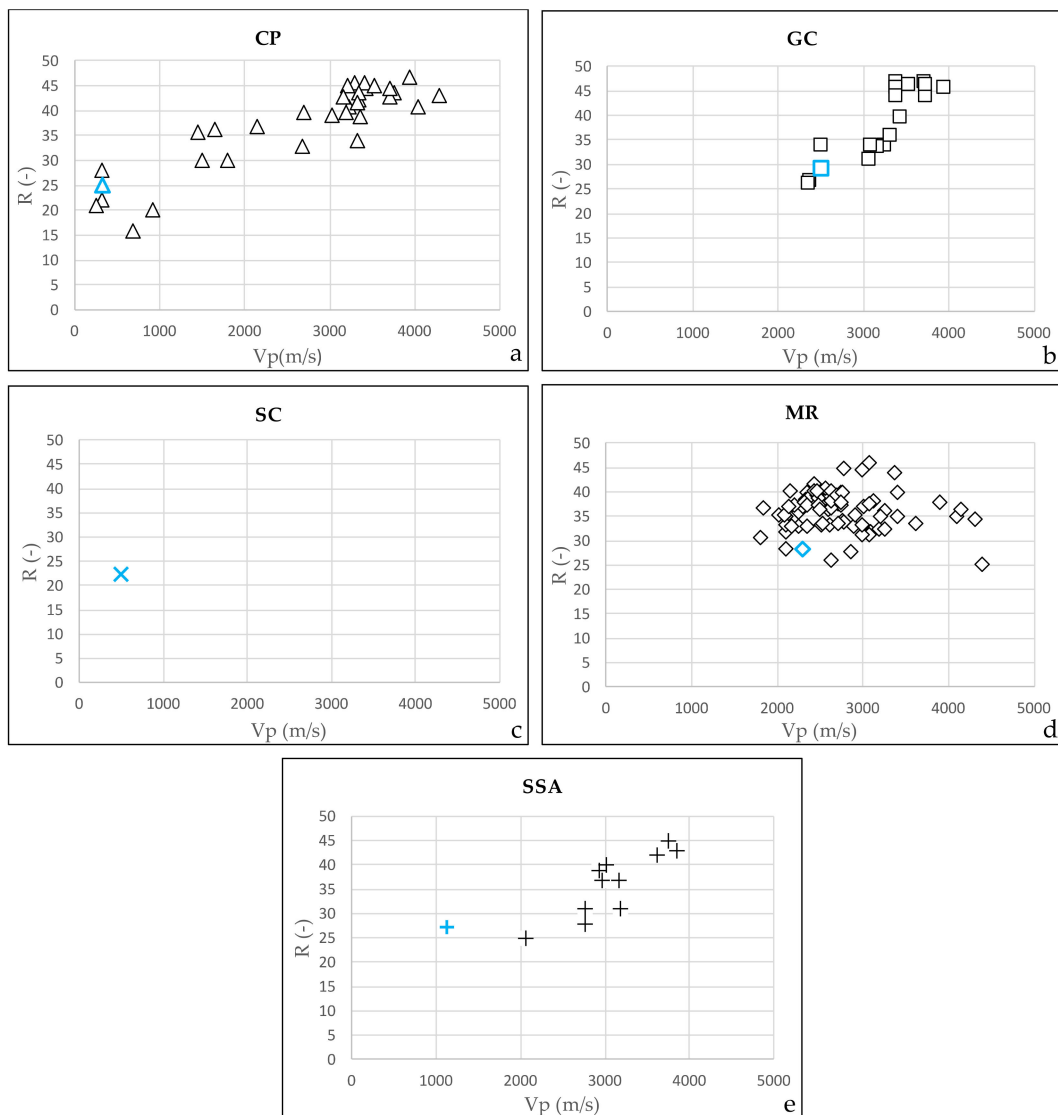


Figure 4. Ultrasonic velocity (V_p) versus rebound values (R). In blue the corbels selected for sampling. Results for (a) Palazzo Corsini Palace, (b) Ginori Conti Palace, (c) Santa Croce Basilica, (d) Medici Riccardi Palace and (e) Santissima Annunziata Basilica, corbels.

Further information about the quality of *Pietra Serena* corbels was provided by calculating the velocity ratio index (VRI) [48]. The index was computed from ultrasonic measurements for the corbels and highlights the strong influence of degradation or fracturing. This methodology has been successfully used on carbonate rocks [49]. The VRI formulation is given below:

$$\text{VRI} = \sqrt{\frac{V_p}{V_L}} \quad (5)$$

where V_p is the wave velocity measured on-site on the corbels and V_L is the velocity of the intact block of *Pietra Serena* (about 4500 m/s, measured in laboratory tests on different quarry blocks). VRI values range from 0 to 1. The block quality was divided into five categories according to VRI as suggested by [48].

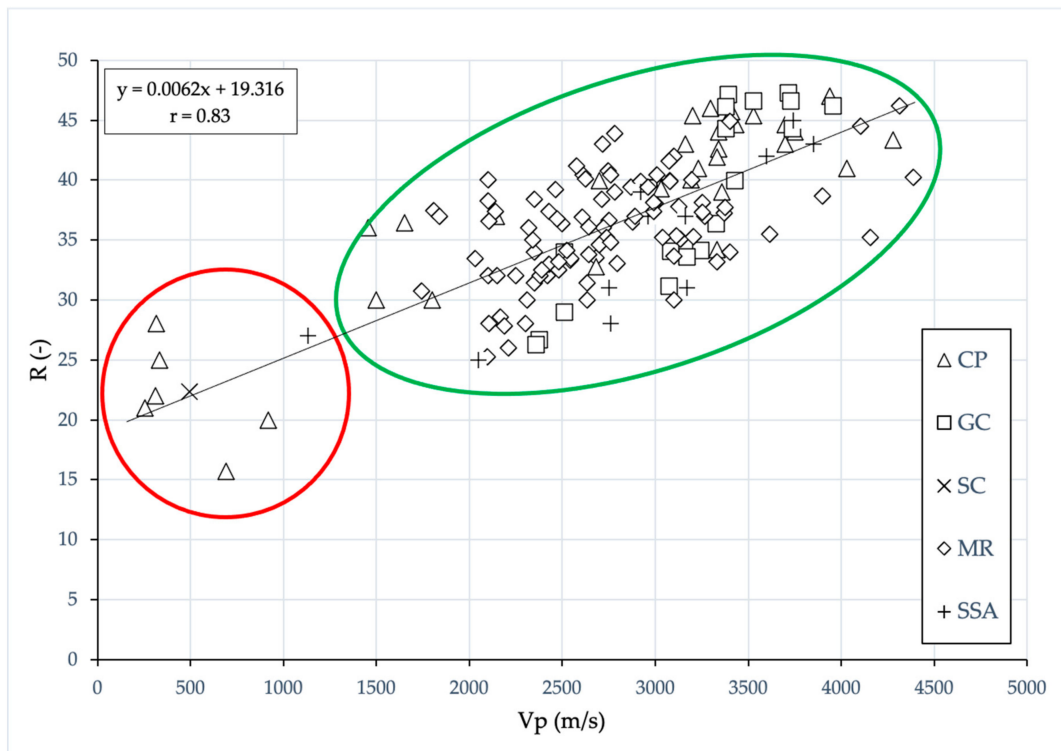


Figure 5. Ultrasonic velocity (V_p) versus rebound values (R) correlation; red cluster represents low V_p and R values corresponding to the most degraded corbels, while the green cluster represents high V_p and R values, which indicate a good state of preservation of *Pietra Serena*.

Figure 6 shows that the stone of SC and several corbels of CP are classified as very poor based on VRI, while all the corbels of GC, MR and SSA are mostly classified as good and very good stones.

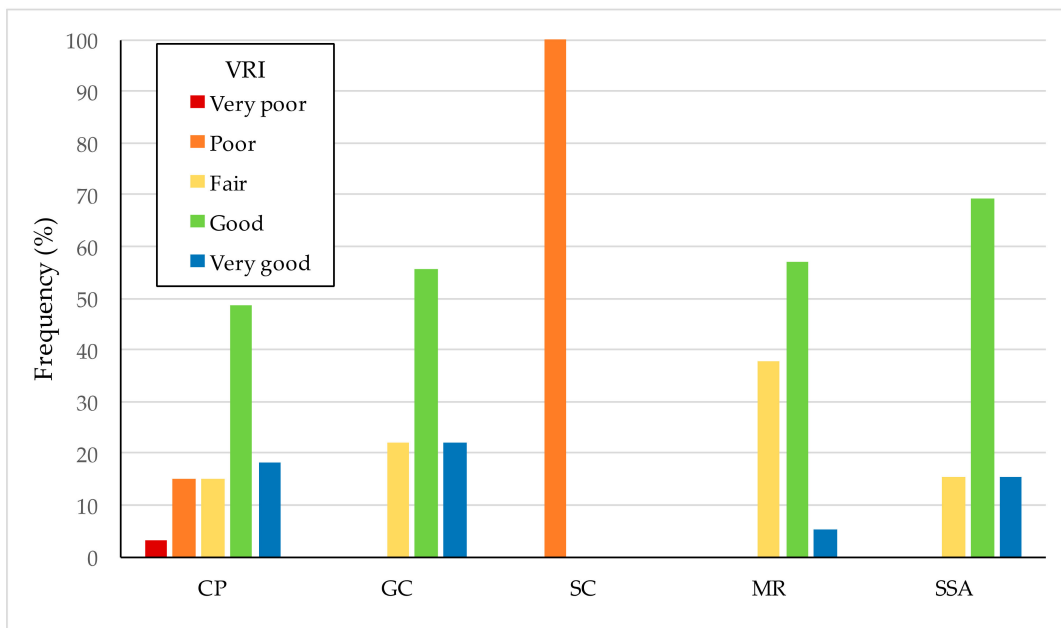


Figure 6. Percentage of *Pietra Serena* corbels of different qualities according to velocity ratio index (VRI).

6. Conclusions

The monitoring of the decay state of *Pietra Serena* used in Florentine historical buildings with NDTs constitutes an important starting point for a database, since it allows for the collection of practical and quick data for restoration and preservation purposes. In this study, several stone corbels placed below balconies and eaves were examined. The proposed methodology was based on the integrated application of mineralogical petrographic, chemical, and physical analysis with ultrasonic and Schmidt hammer tests.

The analyzed samples had mineralogical and petrographic features that suggest that they belonged to different Florentine quarries of the Macigno/Monte Modino Formations. Comparing the physical and chemical analyses with the NDT results, it was possible to identify the five case studies from a dynamic point of view.

The corbels selected for sampling of CP and SC were characterized by both low V_p and R values, in fact it showed a higher porosity and a lower content of CaCO_3 than the other cases. Indeed, this confirmed the high level of decay shown by the macroscopic description.

On the other hand, GC, MR and SSA corbels showed high V_p and R values and were characterized by a higher CaCO_3 content, and low porosity and CI. This demonstrates a good state of conservation of the sandstone elements. This also means that the NDTs results were influenced by the content of CaCO_3 , porosity, and density, all of which change due to the normal environmental decay of the *Pietra Serena*.

All the corbels were investigated with NDTs, in order to obtain a correlation that made it possible to evaluate the on-site state of conservation of the ornamental stone elements. The results showed a good correlation between the V_p and R values, which clearly identified two classes separating the well-preserved corbels from the fallen and the degraded corbels.

A concluding observation is that the quality classification and estimation of decay can be made combining the selected NDTs methods. The results can be used for further investigation as a reference database, to quickly understand the decay state of other *Pietra Serena* ornamental elements. Moreover, the collected data, repeated in time, will allow us to perform a simple and scheduled monitoring of the conditions of the stones.

Author Contributions: Conceptualization, T.S.; data curation, T.S., S.C., I.C., and E.P.; investigation, T.S., S.C. and I.C.; methodology, T.S., S.C., I.C., and E.P.; supervision, E.I. and C.A.G.; writing—original draft, T.S., S.C., I.C., and E.P.; writing—review and editing, E.I. and C.A.G. All authors have read and agreed to the published version of the manuscript.

Funding: This research received no external funding.

Conflicts of Interest: The authors declare no potential conflicts of interest with respect to the research, authorship, and/or publication of this article.

References

1. Brimblecombe, P. *The Effects of Air Pollution on the Built Environment*; Imperial College Press: London, UK, 2003; Volume 2. [[CrossRef](#)]
2. Bonazza, A.; Sabbioni, C.; Ghedini, N. Quantitative data on carbon fractions in interpretation of black crusts and soiling on European built heritage. *Atmos. Environ.* **2005**, *39*, 2607–2618. [[CrossRef](#)]
3. Elyamani, A.; Roca, P. One century of studies for the preservation of one of the largest cathedrals worldwide: A Review. *Sci. Cult.* **2018**, *4*, 1–24. [[CrossRef](#)]
4. Moussa, A. Monitoring building materials exposed to marine environment: Examples from Farasan Islands, Saudi Arabia. *Sci. Cult.* **2019**, *5*, 7–20. [[CrossRef](#)]
5. Vasconcelos, G.; Lourenço, P.; Alves, C.; Pamplona, J. Ultrasonic evaluation of the physical and mechanical properties of granites. *Ultrasonics* **2008**, *48*, 453–466. [[CrossRef](#)]

6. Fais, S.; Cuccuru, F.; Ligas, P.; Casula, G.; Bianchi, M.G. Integrated ultrasonic, laser scanning and petrographical characterisation of carbonate building materials on an architectural structure of a historic building. *Bull. Int. Assoc. Eng. Geol.* **2015**, *76*, 71–84. [[CrossRef](#)]
7. Fioretti, G.; Andriani, G.F. Ultrasonic wave velocity measurements for detecting decay in carbonate rocks. *Q. J. Eng. Geol. Hydrogeol.* **2018**, *51*, 179–186. [[CrossRef](#)]
8. Bozdağ, A.; Ince, I.; Bozdağ, A.; Hatır, M.E.; Tosunlar, M.B.; Korkanç, M. An assessment of deterioration in cultural heritage: The unique case of Eflatunpınar Hittite Water Monument in Konya, Turkey. *Bull. Int. Assoc. Eng. Geol.* **2019**, *79*, 1185–1197. [[CrossRef](#)]
9. Akoglu, K.G.; Kotoula, E.; Simon, S. Combined use of ultrasonic pulse velocity (UPV) testing and digital technologies: A model for long-term condition monitoring memorials in historic Grove Street Cemetery, New Haven. *J. Cult. Herit.* **2020**, *41*, 84–95. [[CrossRef](#)]
10. ICOMOS. *Illustrated Glossary on Stone Deterioration Patterns*; ICOMOS: Paris, France, 2008.
11. Banchelli, A.; Fratini, F.; Germani, M.; Malesani, P.G.; del Manganelli-Fa, C. The sandstones of Florentine historic buildings: Individuation of the marker and determination of the supply quarries of the rocks used in some Florentine monuments. *Sci. Technol. Cult. Herit.* **1997**, *6*, 13–22.
12. Malesani, P.; Pecchioni, E.; Cantisani, E.; Fratini, F. Geolithology and provenance of materials of some historical buildings and monuments in the centre of Florence (Italy). *Episodes* **2003**, *26*, 250–255. [[CrossRef](#)]
13. Fratini, F.; Pecchioni, E.; Cantisani, E.; Rescic, S.; Vettori, S. Pietra Serena: The stone of the Renaissance. *Geol. Soc. Lond. Spéc. Publ.* **2014**, *407*, 173–186. [[CrossRef](#)]
14. Abbate, E.; Bruni, P. Modino–Cervarola o Modino e Cervarola? Torbiditi oligomioceniche ed evoluzione del margine nord appenninico. *Mem. Soc. Geol. Ital.* **1987**, *39*, 19–33.
15. Bruni, P.; Pandeli, E. Il Macigno e le Arenarie di Monte Modino nell’area dell’Abetone. Proceeding of the 76th Riunione estiva S.G.I., L’Appennino Settentrionale, Firenze, Italy, 24–26 September 1992; Guide alle Escursioni Post–Congresso, Escursione 1992; Geological Society: London, UK, 2015; pp. 139–160.
16. Pecchioni, E.; Vettori, S.; Cantisani, E.; Fratini, F.; Ricci, M.; Garzonio, C.A. Chemical and mineralogical studies of the red chromatic alteration of Florentine Pietra Serena sandstone. *Eur. J. Miner.* **2016**, *28*, 449–458. [[CrossRef](#)]
17. Cipriani, N.; Fratini, F.; Nebbiai, M.; Sartori, R. Monte Senario sandstone: Composition, technical characteristics and comparison with the Pietra Serena. In *Arkos: Scienza e Restauro dell’Architettura*; Editinera S.R.L.: Milano, Italy, 2005; pp. 37–44.
18. Cantisani, E.; Garzonio, C.A.; Ricci, M.; Vettori, S. Relationships between the petrographical, physical and mechanical properties of some Italian sandstones. *Int. J. Rock Mech. Min. Sci.* **2013**, *60*, 321–332. [[CrossRef](#)]
19. Winkler, E. Decay of Stone. *Stud. Conserv.* **1971**, *16*, 1–14. [[CrossRef](#)]
20. Malesani, P.P.; Vannucci, S.A. Decay of Pietra Serena e Pietraforte, Florentine building stones: Petrographic observations. *Stud. Conserv.* **1974**, *19*, 36–49.
21. Smith, B.; Gomez-Heras, M.; McCabe, S. Understanding the decay of stone-built cultural heritage. *Prog. Phys. Geogr. Earth Environ.* **2008**, *32*, 439–461. [[CrossRef](#)]
22. Camuffo, D. *Weathering of Building Materials*; World Scientific Pub Co Pte, Lt.: Singapore, 2015; Volume 5, pp. 19–64.
23. Sun, Q.; Dong, Z.; Jia, H. Decay of sandstone subjected to a combined action of repeated freezing–thawing and salt crystallization. *Bull. Int. Assoc. Eng. Geol.* **2019**, *78*, 5951–5964. [[CrossRef](#)]
24. Shariati, M.; Ramli–Sulong, N.H.; Arabnejad, M.M.; Shafiq, P.; Sinaei, H. Assessing the strength of reinforced concrete structures through Ultrasonic Pulse Velocity and Schmidt Rebound Hammer tests. *Sci Res Essays* **2011**, *6*, 213–220.
25. Vasanelli, E.; Sileo, M.; Calia, A.; Aiello, M.A. Non-destructive Techniques to Assess Mechanical and Physical Properties of Soft Calcarene Stones. *Procedia Chem.* **2013**, *8*, 35–44. [[CrossRef](#)]
26. Tandon, R.S.; Gupta, V. Estimation of strength characteristics of different Himalayan rocks from Schmidt hammer rebound, point load index, and compressional wave velocity. *Bull. Int. Assoc. Eng. Geol.* **2014**, *74*, 521–533. [[CrossRef](#)]

27. Morabito, Z.M.; Mazzucato, A.; Tonon, M. Monitoraggio ultrasonico di superfici intonacate. In Proceedings of the 2nd Congresso Nazionale IGIIC, stato dell'arte 2, Genoa, Italy, 27–29 September 2004; p. 78.
28. Sarpün, I.H.; Kılıçkaya, M.S.; Tuncel, S. Mean grain size determination in marbles by ultrasonic velocity techniques. *NDT E Int.* **2005**, *38*, 21–25. [[CrossRef](#)]
29. Sarpün, I.H.; Özkan, V.; Tuncel, S. Determination of mean grain size of various marbles from Turkey by Ultrasonic, attenuation and polarize microscopy methods. In Proceedings of the 5th Pan American Conference for NDT, Cancun, Mexico, 2–6 October 2011; pp. 1–31.
30. Falchi, L.; Zendri, E.; Driussi, G. NDTs in the monitoring and preservation of historical architectural surfaces. In *Emerging Technologies in Non-Destructive Testing VI*; Informa UK Limited: London, UK, 2015; pp. 519–526.
31. Zendri, E.; Falchi, L.; Izzo, F.C.; Morabito, Z.M.; Driussi, G. A review of common NDTs in the monitoring and preservation of historical architectural surfaces. *Int. J. Arch. Heritage* **2017**, *11*, 1–18. [[CrossRef](#)]
32. *ASTM D2845–08 Standard Test Method for Laboratory Determination of Pulse Velocities and Ultrasonic Elastic Constants of Rock*; ASTM International: West Conshohocken, PA, USA, 2008.
33. Goudie, A.S. The Schmidt Hammer in geomorphological research. *Prog. Phys. Geogr. Earth Environ.* **2006**, *30*, 703–718. [[CrossRef](#)]
34. Aydin, A.; Basu, A. The Schmidt hammer in rock material characterization. *Eng. Geol.* **2005**, *81*, 1–14. [[CrossRef](#)]
35. Matthews, J.A.; Owen, G.; Winkler, S.; Vater, A.E.; Wilson, P.; Mourné, R.W.; Hill, J.L. A rock-surface microweathering index from Schmidt hammer R-values and its preliminary application to some common rock types in southern Norway. *Catena* **2016**, *143*, 35–44. [[CrossRef](#)]
36. Sumner, P.; Nel, W. The effect of rock moisture on Schmidt hammer rebound tests on rock samples from Marion Island and South Africa. *Earth Surf. Process. Landf.* **2002**, *27*, 1137–1142. [[CrossRef](#)]
37. Basu, A.; Aydin, A. A method for normalization of Schmidt hammer rebounds values. *Int. J. Rock Mech. Min. Sci.* **2004**, *41*, 1211–1214. [[CrossRef](#)]
38. *ASTM D 5873–00 Standard Test Method for Determination of Rock Hardness by Rebound Hammer Method*; ASTM Stand. International: West Conshohocken, PA, USA, 2001.
39. Debailleux, L. Schmidt hammer rebound hardness tests for the characterization of ancient, fired clay bricks. *Int. J. Arch. Herit.* **2018**, *13*, 288–297. [[CrossRef](#)]
40. *Normal 14/83 Sezioni Sottili e Lucide di Materiali Lapidari: Tecnica di Allestimento*; CNR–ICR: Rome, Italy, 1985.
41. *UNI EN 12407 Natural Stone Test Methods—Petrographic Examination*; Ente Nazionale Italiano di Normazione: Milano, Italy, 2007.
42. *UNI EN 13925 Prove non Distruttive—Diffrazione a Raggi X dai Materiali Policristallini e Amorfi—Parte 1: Principi Generali*; Ente Nazionale Italiano di Normazione: Milano, Italy, 2006.
43. *UNI EN 13925–2 Prove non Distruttive—Diffrazione a Raggi X dai Materiali Policristallini e Amorfi—Parte 2: Procedure*; Ente Nazionale Italiano di Normazione: Milano, Italy, 2006.
44. *UNI EN 13925–3 Prove non Distruttive—Diffrazione a Raggi X dai Materiali Policristallini e Amorfi—Parte 3: Strumenti*; Ente Nazionale Italiano di Normazione: Milano, Italy, 2006.
45. Leone, G.; Leoni, L.; Sartori, F. Revisione di un metodo gasometrico per la determinazione di calcite e dolomite. *Atti. Soc. Tosc. Sci. Nat. Mem.* **1988**, *95*, 7–20.
46. Cantisani, E.; Calandra, S.; Barone, S.; Caciagli, S.; Fedi, M.; Garzonio, C.A.; Liccioli, L.; Salvadori, B.; Salvatici, T.; Vettori, S. The mortars of Giotto's Bell Tower (Florence, Italy): Raw materials and technologies. *Constr. Build. Mater.* **2020**, 120801. [[CrossRef](#)]
47. Calandra, S.; Barone, S.; Cantisani, E.; Fedi, M.; Garzonio, C.A.; Liccioli, L.; Ricci, P. Characterization of mortars of Giotto's Bell Tower for radiocarbon dating in 2019 IMEKO TC-4. In Proceedings of the International Conference on Metrology for Archaeology and Cultural Heritage (MetroArchaeo 2019), Florence, Italy, 4–6 December 2019; pp. 79–83.
48. Kahraman, S.; Ulker, U.; Delibalta, M.S. A quality classification of building stones from P wave velocity and its application to stone cutting with gang saws. *J. S. Afr. I Min. Metall.* **2007**, *107*, 427–430.

49. Cuccuru, F.; Fais, S.; Ligas, P. Dynamic elastic characterization of carbonate rocks used as building materials in the historical city center of Cagliari (Italy). *Q. J. Eng. Geol. Hydrogeol.* **2014**, *47*, 259–266. [[CrossRef](#)]

Publisher’s Note: MDPI stays neutral with regard to jurisdictional claims in published maps and institutional affiliations.



© 2020 by the authors. Licensee MDPI, Basel, Switzerland. This article is an open access article distributed under the terms and conditions of the Creative Commons Attribution (CC BY) license (<http://creativecommons.org/licenses/by/4.0/>).